Kernel-corrected random-phase approximation for the uniform electron gas and jellium surface energy

Adrienn Ruzsinszky, Lucian A. Constantin, and J. M. Pitarke

Phys. Rev. B **94**, 165155 — Published 21 October 2016

DOI: 10.1103/PhysRevB.94.165155

Kernel-Corrected Random-Phase Approximation for the Uniform Electron Gas and Jellium Surface Energy

Adrienn Ruzsinszky,[1] Lucian A. Constantin,[2] and J. M. Pitarke[3,4]

[1] *Department of Physics, Temple University, Philadelphia, PA 19122, USA*
[2] *Center for Biomolecular Nanotechnologies @UNILE, Istituto Italiano di Tecnologia, Via Barsanti, I-73010 Arnesano, Italy*
[3] *CIC nanoGUNE, Tolosa Hiribidea 76, E-20018 Donostia, Basque Country*
[4] *Materia Kondentsatuaren Fisika Saila, DIPC, and Centro Física Materiales CSIC-UPV/EHU, 644 Posta kutxatila, E-48080 Bilbo, Basque Country*

We introduce and test a nonlocal energy-optimized model kernel (NEO) within the adiabatic connection fluctuation-dissipation (ACFD) density-functional theory for the jellium surface and uniform electron gas, as benchmarks for simple metallic systems. Our model kernel is short- ranged for the uniform electron gas paradigm system, and one-electron self-correlation free. One-electron self-interaction freedom is provided by an iso-orbital indicator. We show how several versions of the NEO kernel perform for the uniform electron gas and jellium surface energies, and in addition we explain the underlying physics of self-interaction-free exchange- only kernels for exponentially decaying surface densities.

PACS numbers: 71.10.Ca,71.15.Mb,71.45.Gm

I. INTRODUCTION

Nonempirical density-functional theory (DFT) relies on the knowledge of paradigms.[1] One of these paradigms is the *uniform* electron gas,[2–4] which plays a key role in the construction of many density-functional approximations.[1] The uniform electron gas provides relevant information about correlation in materials and serves as a model for metallic systems.[5] The surface of a *bounded* electron gas, which is different from the bulk, delivers additional information about the ground-state correlation.

As the uniform electron gas has done in the past, the jellium surface can also guide the construction of density functionals. In the jellium model of a simple metal surface, the ions are replaced by a semi-infinite uniform positive background of density n, which is neutralized by a valence electron density $n(z)$ allowed to leak out into the vacuum side of the surface.

The accuracy of[6–8] local and semilocal density functionals is limited by the approximating form of the exchange-correlation (xc) energy or its corresponding potential[9]. Density-functional approximations are usually benchmarked against correlated wave-function based methods[10–15]. Approximations that rely on the concept of the slowly-varying limit of the perturbed uniform electron gas deliver accurate lattice properties[16]. The simplest approximation, the local density approximation (LDA)[3], is reasonably accurate for periodic solids[17]. Generalized gradient approximations (GGAs) utilize information about slowly-varying densities[18–22]. These GGAs have proven accurate for both bulk solids and surfaces. Meta-GGAs beyond the GGA level add the positive kinetic-energy density as a new ingredient to the existing electron density and density gradient in GGAs[23–29]. With all these ingredients, the meta-GGA density functionals are the potentially most accurate semilocal approximations, with the flexibility to describe bulk solids, surfaces, and molecules at the same time[29,30]. Adiabatic-connection fluctuation-dissipation (ACFD) approximations [the random-phase approximation (RPA) in particular] stand on the fifth and highest rung of a ladder[31] of density-functional approximations, employing the unoccupied as well as the occupied Kohn-Sham (KS) orbitals in a fully nonlocal way that can potentially solve problems such as capturing weak van-der-Waals interactions[32] and static correlation for the H_2 molecule in a spin-restricted formalism[33].

Jellium surface energies were thoroughly investigated within an ACFD approach[34–37], and these results were compared to Fermi-hypernetted chain (FHNC)[13] and Diffusion-Monte- Carlo (DMC) surface energies[14,15]. Later, Yan *et al.* made an assessment of several density-functional approximations to the jellium surface energy[38]. Many refinements of DFT (including ACFD), as summarized in Ref. 39, produced jellium surface energies close to those obtained in the LDA and thus much lower than those of FHNC and early DMC[14]. A more recent DMC calculation[40] agrees well with the DFT values.

By combining an adiabatic-connection (AC) formula with the fluctuation-dissipation (FD) theorem, one obtains an *exact* expression for the xc energy of an arbitrary many-electron system (unless stated otherwise, atomic units are used throughout):[41]

$$E_{xc} = \frac{1}{2}\int_0^1 d\lambda \int d\mathbf{r} \int d\mathbf{r}' v(\mathbf{r},\mathbf{r}') \left\{ \left[-\frac{1}{\pi}\int_0^\infty d\omega \times \chi_\lambda(\mathbf{r},\mathbf{r}',\mathrm{i}\omega)\right] - n(\mathbf{r})\delta(\mathbf{r}-\mathbf{r}')\right\}, \quad (1)$$

where $v = 1/|\mathbf{r}-\mathbf{r}'|$ is the bare Coulomb interaction and χ_λ represents the interacting density-response function of a *fictitious* many-electron system with the electron-electron interaction strength λe^2. In the framework of time-dependent DFT (TDDFT), the interacting density-

response function χ_λ obeys a Dyson-like integral equation:[42]

$$\chi_\lambda = [1 - \chi_0(\lambda\, v + f_{xc}^\lambda)]^{-1}\chi_0, \tag{2}$$

where χ_0 is the density-response function of non-interacting KS electrons. The RPA sets the xc kernel $f_{xc}^\lambda(\mathbf{r}, \mathbf{r}', \omega)$ to zero. In much of this work, we will need only the exchange-only ($\lambda = 0$) kernel, but we will leave λ general in the notation. In the RPA, Eqs. (1) and (2) are combined, bootstrapping a crude approximation for χ_λ to a more sophisticated one for E_{xc}.[43] For the uniform electron gas, it was shown[44] that an adiabatic (static) local kernel overshoots the correlation energy by about as much ($\sim$0.5 eV) as the RPA undershoots it; a static nonlocal kernel[45,46] was found to reduce the error to $\sim$0.1 eV, and a dynamic nonlocal kernel[47] was found to reduce the error down to $\sim$0.02 eV.

There are other routes to correct for the missing short-range correlation. The quantum chemistry community often uses the second-order screened exchange (SOSEX) contribution (coming from the wave-function anti-symmetry)[48]. The SOSEX correction was found to perform somewhat controversially in quantum chemistry.

The first implementation of the ACFD scheme for a non-uniform system was reported in Ref. 34 for the jellium surface. Although RPA delivers too deep correlation energy for the short- range, jellium surface energies are surprisingly accurate. The better performance of RPA for the jellium surface energy was explained by the relevance of the long-range correlation for surfaces. Even if RPA does not provide an accurate short-range correlation, the error tends to cancel out the surface energy. Therefore exchange-correlation kernels, which can correct the deep RPA correlation for short-range in bulks or inhomogeneous systems, do not give much contribution for the jellium surface energy. The same conclusion can be drawn when the correction to the RPA called RPA+ is applied to the jellium surface. For energy differences in processes that conserve the electron number, it was argued[38] that the correction from RPA+, although large for the total energy (about +0.5 eV per electron), tends to cancel out almost completely. Beyond the jellium model, recent calculations showed a remarkably accuracy of the RPA for various properties (including the surface energy) of real materials[49–55].

To account for this missing short-range part of the RPA correlation energy in the uniform electron gas and inhomogeneous systems, we rely on (for the jellium surface) a nonlocal energy- optimized (NEO) model kernel[56,57] which has been introduced and tested recently[58]. This kernel is designed to satisfy exact constraints utilizing the iso-orbital Z indicator, a meta-GGA ingredient. The original construction of NEO was designed to produce a correctly long-ranged ($\sim 1/u$) exchange kernel for one- and two-electron systems, where $Z = 1$. A problem arises that it also produces a long-ranged exchange kernel in the tail of the density of a jellium surface, since $Z \to 1$ and $k_F \to 0$ there. (Here $k_F = (3\pi^2 n)^{1/3}$ is the Fermi wave vector.) In this work we present the NEO kernel and test it for the jellium surface. Along with the original NEO kernel, we also introduce a modification of the original expression to restore the correct decay of the density tail for the jellium surface. With this construction the NEO-kernel- corrected RPA should be correct at long range, as pointed out by Ref. 34.

II. COMPUTATIONAL FRAMEWORK

Consider a many-electron system that is neutralized by a uniform positive background (jellium) of density $\bar{n}$ cut off sharply at a planar surface (at $z = z_0$). The xc surface energy is obtained as follows[35]

$$\sigma_{xc} = \frac{N}{A}\left\{\varepsilon_{xc}[n] - \varepsilon_{xc}^{unif}(\bar{n})\right\}, \tag{3}$$

where $\varepsilon_{xc}[n]$ and $\varepsilon_{xc}^{unif}(\bar{n})$ represent, respectively, the xc energy per particle of the actual semi-infinite many-electron system [of density $n(z)$] and a uniform electron gas (of density $\bar{n}$) cut off sharply at $z = z_0$; here, $\bar{n} = k_F^3/(3\pi^2)$, k_F being the magnitude of the bulk Fermi wavevector. Using Eq. (1), one finds:

$$\varepsilon_{xc}[n] = \int_0^\infty d(q/k_F)\, \varepsilon_{xc,q}[n], \tag{4}$$

where

$$\varepsilon_{xc,q}[n] = \frac{k_F}{4\pi}\int dz \int dz' n(z)\, v_q(|z - z'|)[-\frac{1}{\pi n(z)} \times \int_0^1 d\lambda \int_0^\infty d\omega \chi_\lambda(z, z'; q, i\omega) - \delta(z - z')]. \tag{5}$$

Here, q represents the magnitude of a two-dimensional (2D) wavevector parallel to the surface, $v_q(|z-z'|)$ is the 2D Fourier transform of the bare Coulomb interaction v, and $\chi_\lambda(z, z'; q, i\omega)$ is the 2D Fourier transform of the interacting density-response function χ_λ of Eq. (2). If the interacting density-response function χ_λ is replaced for all λ by the non-interacting density response function χ_0, then Eq. (5) reduces to the exact exchange energy per particle $\varepsilon_{x,q}[n]$. We define the correlation energy per particle $\varepsilon_{c,q}[n] = \varepsilon_{xc,q}[n] - \varepsilon_{x,q}[n]$.

For $\varepsilon_{xc}^{unif}(\bar{n})$, one simply needs to replace (i) the interacting density-response function $\chi_\lambda(z, z'; q, i\omega)$ entering Eq. (5) by that of a uniform electron gas and (ii) the electron density $n(z)$ [also entering Eq. (5)] by the step function $\bar{n}\,\theta(z_0 - z)$. This yields a 2D wavevector analysis [Eq. (4)] of the uniform-gas xc energy per particle $\varepsilon_{xc}^{unif}(\bar{n})$, which will be needed below for a 2D wavevector analysis of the xc surface energy. Alternatively, one can use Eq. (1) to reach the following *three-dimensional* (3D) wavevector analysis:

$$\varepsilon_{xc}^{unif}(\bar{n}) = \int_0^\infty d(Q/k_F)\, \varepsilon_{xc,Q}^{unif}(\bar{n}), \tag{6}$$

where

$$\varepsilon_{xc,Q}^{unif}(\bar{n}) = \frac{k_F}{4\pi^2} v_Q \left[-\frac{1}{\pi \bar{n}} \int_0^1 d\lambda \int_0^\infty d\omega \chi_\lambda(Q, i\omega) - 1 \right]. \quad (7)$$

Here, Q represents the magnitude of a 3D wavevector, v_Q is the 3D Fourier transform of the bare Coulomb interaction v, and $\chi_\lambda(Q, i\omega)$ is the 3D Fourier transform of the interacting density-response function χ_λ [see Eq. (2)] of a uniform electron gas of density $\bar{n}$.

For the numerical calculations reported here, we start with a jellium slab of finite width along the z direction, and we then take the limit of large thickness. In this work we used the code described in Refs.[34,35,59], that computes numerically Eqs. (3)-(5) using accurate (occupied and unoccupied) LDA orbitals[35]. Instead of considering the double-cosine Fourier representation of the density-response function (as done in Ref.[35]), we worked directly in the z-space. This approach simplifies considerably the computational implementation of the kernels, but needs a large number of grid points in the z-direction, in order to obtain converged results (up to 1100 z-points on a Gaussian grid).

III. METHODOLOGY

A. The NEO-I kernel

Here we invoke NEO: a nonlocal energy-optimized model kernel[56,57] which has been introduced and tested recently for the uniform electron gas.[58] This kernel (which can be applied to an arbitrary non-uniform system) is based on exact constraints and on the concept of the uniform electron gas;[44] the most widely-applicable approximations of DFT and TDDFT are well known to rely on this paradigm. The NEO kernel, as introduced in Ref. 58 (NEO-I), is:

$$f_{xc}^{\lambda,\mathrm{NEO}}([n], \mathbf{r}, \mathbf{r}') = -\lambda v(\mathbf{r}, \mathbf{r}') \sum_\sigma \left(\frac{n_\sigma}{n}\right)^2 \times \mathrm{erfc}(a^{\mathrm{NEO-I}} |\mathbf{r} - \mathbf{r}'|), \quad (8)$$

where

$$a^{\mathrm{NEO-I}} = \sqrt{\tilde{c}(1 - Z_\sigma^2)}\, k_{F\sigma}, \quad (9)$$

$Z_\sigma = \tau_\sigma^W / \tau_\sigma$ being a meta-GGA ingredient,[24,25] τ_σ being the KS kinetic-energy density

$$\tau_\sigma = \frac{1}{2} \sum_\alpha^{occup} |\nabla \phi_{\alpha\sigma}|, \quad (10)$$

and $\tau_\sigma^W = |\nabla n_\sigma|^2/(8n_\sigma)$ being the von Weizsäcker kinetic-energy density[60] (which equals τ_σ for one- and two-electron ground states). The decaying function erfc is the complementary error function, n_σ and n are the σ spin and the total electron density, respectively, and $k_{F\sigma} = (6\pi^2 n_\sigma)^{1/3}$. These quantities are all evaluated at $(\mathbf{r} + \mathbf{r}')/2$.

For one-electron densities, one finds the expected result $f_{xc}^{\lambda,\mathrm{NEO}} = -\lambda v$. For two electrons in a spin singlet, one finds the exact-exchange form $f_{xc}^{\lambda,NEO} = -\lambda v/2$, which is exact in the high-density limit. In the short-range limit, the NEO-I kernel becomes $-\lambda v \sum_\sigma (n_\sigma/n)^2$ as does the PGG kernel;[61] in the spin-polarized case, this further simplifies to $-\lambda v$, while in the spin-unpolarized case it becomes $-\lambda v/2$. In the long-range limit, $f_{xc}^{\lambda,\mathrm{NEO}}$ vanishes rapidly, except in the one- and two-electron regions. The exact xc kernel of the uniform electron gas is known to be nonlocal but short-ranged, and the NEO-I kernel has these features.

The $\tilde{c}$ parameter entering Eq. (9) is taken to fit the exact second-order exchange contribution to the uniform-gas correlation energy, which can be evaluated from explicit expressions given by Langreth and Perdew[41] and by von Barth and Hedin[62]; one finds $\tilde{c} = 0.264$, which makes a large improvement over the RPA ($\tilde{c} \to \infty$).

B. NEO-II kernel

The NEO-I kernel of Eqs. (8)-(9) is simply the bare Coulomb interaction λv multiplied by a decaying function of the variable $a^{\mathrm{NEO-I}}|\mathbf{r} - \mathbf{r}'|$. This is designed in order to (i) produce a correctly long-ranged exchange kernel for one- and two-electron systems, where $Z_\sigma = 1$, and (ii) produce no second-order gradient correction to the RPA correlation energy in a slowly-varying high electron density, where $Z_\sigma \to 0 + \mathcal{O}(\nabla^2)$. The problem is that this kernel (as introduced in Ref. 58) produces an unwanted long-ranged exchange kernel in the tail of the electron density of a jellium surface ($Z_\sigma \to 1$ and $k_{F\sigma} \to 0$) where the RPA should be recovered as discussed in Ref. 35. Hence, here we replace Eq. (9) by

$$a^{NEO-II} = \sqrt{\tilde{c}(3\alpha_\sigma - 3\alpha_\sigma^2 + \alpha_\sigma^3)}\, k_{F\sigma}, \quad (11)$$

where $\alpha_\sigma = (\tau_\sigma - \tau_\sigma^W)/\tau_\sigma^{unif}$, τ_σ^{unif} being the Thomas-Fermi kinetic-energy density:[63,64]

$$\tau_\sigma^{unif} = (1/2)(3/10)(3\pi^2)^{2/3}(2n_\sigma)^{5/3}. \quad (12)$$

This new approach (NEO-II) represents a clear improvement, as it leaves *unchanged* the correct behavior of the NEO-I kernel for one- and two-electron densities (at $\alpha_\sigma = 0$) and also for slowly-varying densities [at $\alpha_\sigma = 1 + \mathcal{O}(\nabla^2)$] and kills, at the same time, the unwanted kernel in the tail of the electron density far away from the surface (at $\alpha_\sigma \to \infty$). As one moves from NEO-I to NEO-II, the parameter $\tilde{c}$ does not need to be refitted.

By construction, for α values that are close to 1 (slowly-varying densities) the coefficient $3\alpha_\sigma - 3\alpha_\sigma^2 + \alpha_\sigma^3$ entering Eq. (11) deviates little from unity, so the range of our NEO-II kernel is of the order of k_F^{-1}. Hence, over this range of α values the kernel correction to RPA is

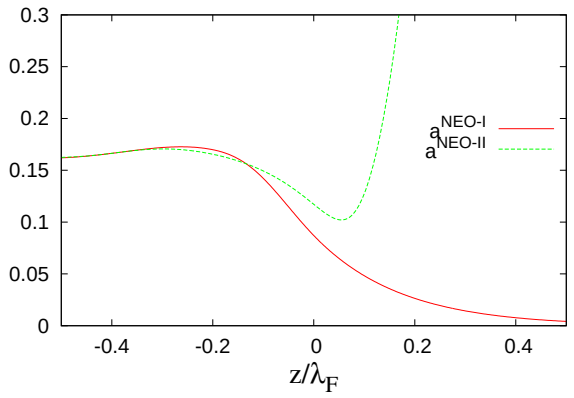

FIG. 1. The coefficients a^{NEO-I} and a^{NEO-II} defining the kernels NEO-I and NEO-II, for a jellium surface with the electron-density parameter $r_s = 6$. The surface is at $z = 0$, the bulk is at $z < 0$, and the vacuum is at $z > 0$.

nearly local, as in the semilocal correction to RPA of Yan, Kurth, and Perdew.[38]

In Fig. 1, we show a comparison between the coefficients a^{NEO-I} and a^{NEO-II} defining the kernels NEO-I and NEO-II, for a jellium surface with the electron-density parameter $r_s = 6$. By construction, these functions agree well in the bulk and even at the surface, while in the vacuum side far from the surface one finds: $a^{NEO-I} \to 0$ and $a^{NEO-II} \to \infty$, as expected. The quantity α we are introducing here represents a kinetic-energy dependent ingredient that plays a key role in the construction of meta-GGA functionals[27,28,65–68] and is also relevant for a correct asymptotic description of the electron density.[69,70] Note, for example, that $1/\left[1+\alpha(\mathbf{r})^2\right]$ is the electron-localization function often used in the characterization of chemical bonds.[71,72]

C. NEO-III kernel

One of the ingredients of the NEO-I kernel [the parameter $\tilde{c}$ entering Eq. (9)] is constructed to fit the exact second-order exchange contribution to the uniform-gas correlation energy. Now we construct NEO-III by replacing the coefficient a^{NEO-I} by the new coefficient

$$a^{NEO-III} = \sqrt{\frac{\tilde{c}}{1+br_s^c}(1-Z_\sigma^2)k_{F\sigma}}, \qquad (13)$$

where the energy-optimization coefficient $\tilde{c}$ entering Eq. (9) has been replaced by the new electron-density dependent coefficient $\tilde{c}/(1+br_s^c)$, with the parameters $b = 1.1$ and $c = 1.35$ taken to fit the PW92[73] correlation energy for electron densities down to $r_s = 1000$.

We do not tried to construct the analog of Equation (13) using α instead of Z. Z and α in NEO-I, and NEO-II present different physics in the density tail, while the replacement of $\tilde{c}$ by $\sqrt{\frac{\tilde{c}}{1+br_s^c}}$ in NEO-III was designed to test the applicability of the kernel for density regions which are different from high-densities.

TABLE I. Correlation energy of the uniform electron gas (in mHa), as obtained from Eq. (1) with the use of the NEO-I and NEO-III kernels, for various values of the electron-density parameter r_s. For the uniform electron gas, the kernels NEO-I and NEO-II coincide. The PW92 correlation energy[73] is given for comparison. The values in parenthesis are relative deviations from the exact (PW92) values. The last line reports the root mean square (RMS).

r_s	NEO-I	NEO-III	exact (PW92)
1	-65.12 (-0.0895)	-60.29 (-0.0087)	-59.77
2	-50.56 (-0.1296)	-44.08 (0.0152)	-44.76
3	-42.92 (-0.1619)	-36.34 (0.0162)	-36.94
4	-37.93 (-0.1901)	-31.76 (0.0035)	-31.87
5	-34.33 (-0.2165)	-28.65 (-0.0152)	-28.22
6	-31.55 (-0.2407)	-26.37 (-0.0369)	-25.43
10	-24.60 (-0.3247)	-20.90 (-0.1255)	-18.57
100	-6.50 (-1.0376)	-6.12 (-0.9185)	-3.19
1000	-1.31 (-2.3590)	-1.29 (-2.3077)	-0.39
RMS	5.351	1.374	

In Table I, the uniform-gas correlation energy is given for various values of r_s, as obtained with the use of the NEO-I (or NEO-II) and NEO-III kernels. NEO-III correlation energy shows reduced deviations for each r_s compared to NEO-I. This fact indicates that NEO-III is performing better for the integrated correlation energies of individual r_s values. This is not surprising since the parameters in NEO-III were obtained by fitting to the uniform electron gas over a wide range of densities. Notice that the better correlation energies in NEO-III show up in the wavevector analysis of Fig. 2 only in the correlation energy, as an integrated area under the curve.

IV. RESULTS AND DISCUSSION

Figure 2 exhibits the Q-dependent correlation energy per particle $\varepsilon_{c,Q}^{unif}(\bar{n})$ (3D wavevector analysis) of a uniform electron gas with $r_s = 2$ and $r_s = 5$, as obtained from Eq. (7). In the long-wavelength ($Q \to 0$) limit, where the RPA is exact, all calculations converge, as expected. At moderate values of Q, NEO-I agrees very well with the Perdew-Wang parametrization[74] in a region where RPA starts to deviate significantly. At the shortest wavelengths, all kernel-corrected calculations improve considerably over the RPA, although they give Q-dependent correlation energies that are still below the exact calculation.

Since both NEO-I and NEO-II kernels were fitted against the second-order exchange energy, they both have

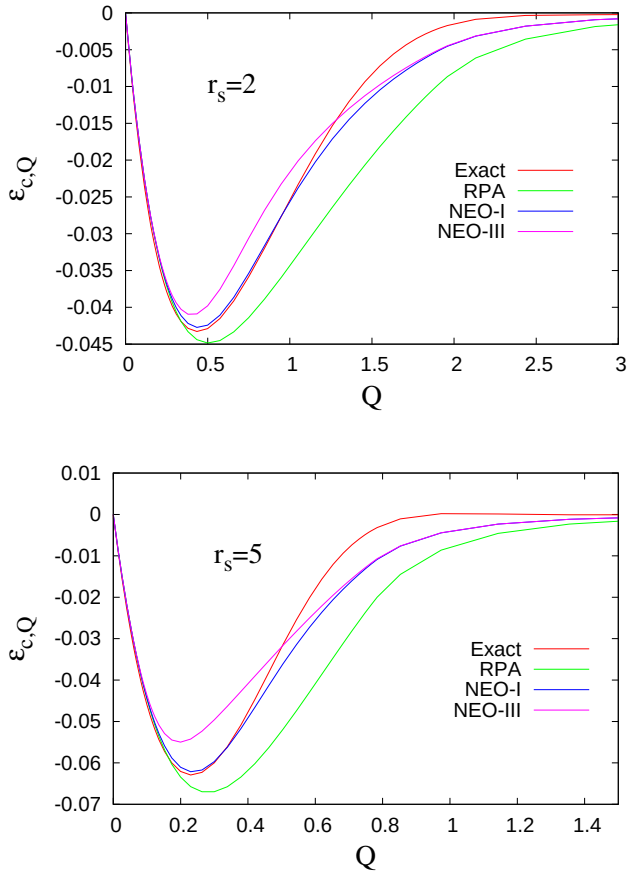

FIG. 2. 3D wavevector analysis of the correlation energy per particle $\varepsilon_{c,Q}^{unif}(\bar{n})$ of a uniform electron gas with $r_s = 2$ and $r_s = 5$, as obtained from Eq. (7) in the RPA and with the use of the NEO-I and NEO-III kernels. The same quantity, as obtained from the Perdew-Wang parametrization of the uniform-gas correlation-hole density[74] (exact) is given for comparison. For the uniform electron gas, the kernels NEO-I and NEO-II coincide.

the same physics built in for the high-density limit. In Ref. 58 one of the authors has shown that for r_s between 1 and 20, the fitted parameter produces a distribution of errors compared to PW92 between approximately 3 and 5 mHa. Small displacement below and above this fitted parameter delivers a balance of small absolute errors and small distribution of error over a large range of densities. Therefore this particular fitting provides some flexibility for the kernel to be accurate in both high-density and lower density regions as well. The balance of good absolute errors and error distribution transfers to the wavevector analysis by tuning the agreement for small to intermediate Q without changing $\tilde{c}$. NEO-III is worst than NEO-I for intermediate wavevectors, but its integrated correlation energies are better.

Figure 3 shows the q-dependent correlation energy per particle $\varepsilon_{c,q}[n]$ (2D wavevector analysis) of a jellium slab of width $a = 2.23\lambda_F$ ($\lambda_F = 2\pi/k_F$ is the Femi wavelength) and $r_s = 2.07$ (the electron-density parameter corresponding to valence electrons in Al), as obtained from Eq. (5). Here we compare our RPA and beyond-RPA calculations to the inhomogeneous Singwi-Tosi-Land-Sjölander (ISTLS) calculations reported in Ref. 39. As in the case of the uniform electron gas, all calculations converge, as expected, in the long-wavelength ($q \to 0$) limit. At moderate values of q, both NEO-I and NEO-II agree well with our reference calculation (ISTLS) in a region where RPA starts to deviate significantly. At the shortest wavelengths, all kernel-corrected calculations are slightly below our reference calculation (ISTLS), as occurs in the case of the uniform electron gas. The best results here (compared to the ISTLS reference) are obtained by using the NEO-I and NEO-II kernels.

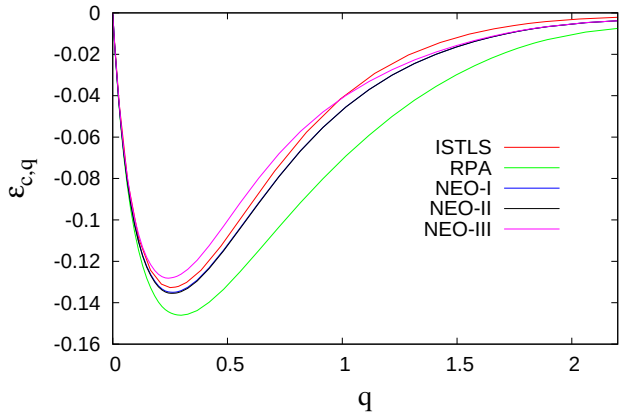

FIG. 3. 2D wavevector analysis of the correlation energy per particle $\varepsilon_{c,q}[n]$ of a jellium slab of width $a = 2.23\lambda_F$ and $r_s = 2.07$, as obtained from Eq. (5) in the RPA and with the use of the NEO-I, NEO-II, and NEO-III kernels. ISTLS calculations (see Ref. 39) are given for comparison.

In Fig. 4, we show (for $r_s = 2.07$) our wavevector analysis of the jellium surface energy

$$\gamma_{c,q} = (N/A)\left\{\varepsilon_{c,q}[n] - \varepsilon_{c,q}^{unif}(\bar{n})\right\}, \qquad (14)$$

where N is the total number of electrons and A represents a normalization area. The area under each curve represents the correlation surface energy σ_c, which we give in Table II. All NEO kernels yield accurate jellium surface energies, which are (i) close to the ISTLS calculation and (ii) within the error bar of DMC calculations.

Figure 4 shows that in the long-wavelength ($q \to 0$) limit all calculations coincide with the RPA calculation, which is exact in this limit. In the large-q limit, where the RPA fails badly, all kernel-corrected calculations agree with each other and with our reference calculation (ISTLS); this is an expected result, since all calculations yielding accurate uniform-gas correlation energies are expected to also yield an accurate γ_q in this region.[36] Differences among our kernel-corrected calculations and between these calculations and our reference calculation

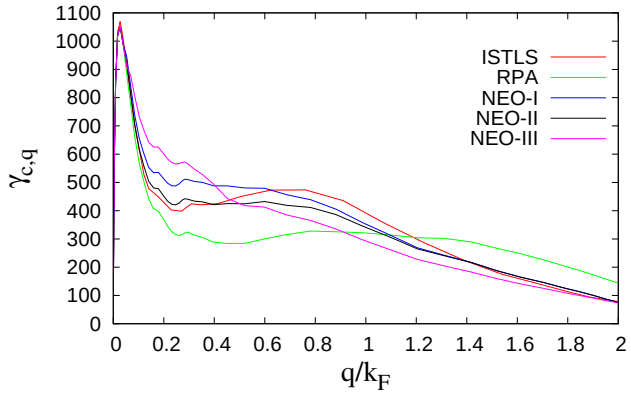

FIG. 4. 2D wave-vector analysis $\gamma_{c,q}$ of the correlation surface energy of a jellium slab of width $a = 2.23\lambda_F$ and $r_s = 2.07$. The area under each curve represents the corresponding correlation surface energy σ_c. Units are erg/cm^2 (1 hartee/bohr^2 $= 1.557 \times 10^6$ erg/cm^2).

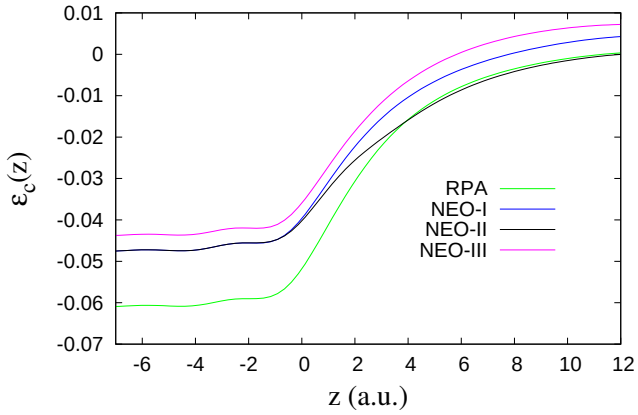

FIG. 5. Correlation energy per particle (ε_c versus z, for a jellium slab of width $a = 2.23\lambda_F$ and $r_s = 2.07$. The surface is at $z = 0$, the bulk is at $z < 0$, and the vacuum is at $z > 0$.

TABLE II. NEO-I, NEO-II, and NEO-III correlation surface energies σ_c of a jellium surface with $r_s = 2.07$. LDA, PBEsol, ISTLS,[39] and DMC[40] correlation energies are given for comparison. NEO and ISTLS calculations represent the surface energy of a *semi-infinite* jellium, which has been obtained from finite-slab calculations by following the extrapolation procedure described in Ref. 35. Units are erg/cm^2 (1 hartee/bohr^2 $= 1.557 \times 10^6$ erg/cm^2).

r_s	LDA	PBEsol	NEO-I	NEO-II	NEO-III	ISTLS	DMC
2.07	287	645	702	692	714	730	697± 45

(ISTLS) arise at intermediate values of q. The NEO-II kernel yields correlation energies γ_q that are very close to our reference calculation (ISTLS) for wavevectors up to $q \approx 0.4$. This is an expected result, since this is the only kernel that is free from an unrealistic long-ranged behavior in the tail of the electron density into the vacuum side of the surface. At larger values of q the NEO-II kernel yields correlation energies that are slightly below the ISTLS result, thus leading to a total NEO-II surface energy that is slightly smaller than the ISTLS surface energy.

We close this paper by looking at the position-dependent xc energy per particle $\varepsilon_{xc}([n], z)$, which for a many-electron system that is invariant in two directions we define as follows[59]

$$E_{xc} = A \int dz\, n(z)\, \varepsilon_{xc}([n], z), \tag{15}$$

E_{xc} being the xc energy of Eq. (1). Equation (15) itself does not define $\varepsilon_{xc}([n], z)$ uniquely[75–77], but here we use the choice made in Equation (1).

Figure 5 exhibits the correlation energy per particle $\varepsilon_c([n], z)$. Only the NEO-II kernel is found to capture both the correct $\varepsilon_c([n], z)$ in the bulk (which in the case of the RPA is too negative) and the correct image-like $\varepsilon_c([n], z)$ far away from the surface (where the RPA is exact[59] and NEO-I and NEO-III are all wrong). This is an expected result, since the NEO-I and NEO-III kernels produce an unwanted long-ranged behavior in the tail of the electron density due to the inability of the Z ingredient entering Eq. (9) to distinguish between the surface tail and one- or two-electron regions. The relevance of the α parameter versus Z was mentioned in the context of orbital overlap in closed-shell species .[27,29,78]

V. CONCLUSIONS

We have constructed a nonlocal energy-optimized model kernel[56,57] with various inhomogeneity parameters, which we have tested for the jellium-surface problem. Our work reveals the role and significance of α, a dimensionless deviation from the single orbital shape, as an ingredient for exponentially decaying surface densities.

A kernel-corrected RPA calculation of the xc jellium surface energy was reported in Ref. 36. In Ref. 36, the xc kernel $f_{xc}^{\lambda}(\mathbf{r}, \mathbf{r}', \omega)$ was taken to be (by assuming that the electron density variation is small within the short range of the kernel) equal to the xc kernel of a uniform electron gas of density $[n(\mathbf{r}) + n(\mathbf{r}')]/2$. Krotscheck and Kohn,[13] however, had argued that this local-density approximation for the particle-hole interaction might be inadequate to calculate the surface energy of simple metals. The present work brings us to the conclusion that the use of an appropriate kernel (like NEO-II), which does not only depend on the electron density at $(\mathbf{r} + \mathbf{r}')/2$ but also on its gradient as well as the kinetic energy density, does not change the jellium surface energy significantly compared to the RPA value, and leaves it close to our reference

ISTLS and DMC calculations.

VI. ACKNOWLEDGMENT

A.R. acknowledges the support of the National Science Foundation under Grant No.DMR-1553022. We thank Prof. J. P. Perdew for many stimulating and enjoyable discussions.

[1] J. P. Perdew, A. Ruzsinszky, J. Tao, V. N. Staroverov, G. E. Scuseria, and G. I. Csonka, J. Chem. Phys. **123**, 062201 (2005).
[2] P. Hohenberg and W. Kohn, Phys. Rev. **136**, B864 (1964).
[3] W. Kohn and L. J. Sham, Phys. Rev. **140**, A1133 (1965).
[4] S. Ichimaru, Rev. Mod. Phys. **54**, 1017 (1982).
[5] C. Kittel, *Introduction to solid state physics* (Wiley, 2005).
[6] N. D. Lang and W. Kohn, Phys. Rev. B **1**, 4555 (1970).
[7] N. D. Lang and W. Kohn, Phys. Rev. B **3**, 1215 (1971).
[8] N. D. Lang and W. Kohn, Phys. Rev. B **7**, 3541 (1973).
[9] J. P. Perdew and K. Schmidt, AIP Conference Proceedings **577**, 1 (2001).
[10] Z. Y. Zhang, D. C. Langreth, and J. P. Perdew, Phys. Rev. B **41**, 5674 (1990).
[11] D. C. Langreth and M. J. Mehl, Phys. Rev. Lett. **47**, 446 (1981).
[12] J. P. Perdew, K. Burke, and M. Ernzerhof, Phys. Rev. Lett. **77**, 3865 (1996).
[13] E. Krotscheck, W. Kohn, and G.-X. Qian, Phys. Rev. B **32**, 5693 (1985).
[14] X.-P. Li, R. J. Needs, R. M. Martin, and D. M. Ceperley, Phys. Rev. B **45**, 6124 (1992).
[15] P. H. Acioli and D. M. Ceperley, Phys. Rev. B **54**, 17199 (1996).
[16] J. P. Perdew, L. A. Constantin, E. Sagvolden, and K. Burke, Phys. Rev. Lett. **97**, 223002 (2006).
[17] F. Tran, J. Stelzl, and P. Blaha, J. Chem. Phys. **144**, 204120 (2016).
[18] R. Armiento and A. E. Mattsson, Phys. Rev. B **72**, 085108 (2005).
[19] J. P. Perdew, A. Ruzsinszky, G. I. Csonka, O. A. Vydrov, G. E. Scuseria, L. A. Constantin, X. Zhou, and K. Burke, Phys. Rev. Lett. **100**, 136406 (2008).
[20] Z. Wu and R. E. Cohen, Phys. Rev. B **73**, 235116 (2006).
[21] Y. Zhao and D. G. Truhlar, J. Chem. Phys. **128**, 184109 (2008).
[22] L. A. Constantin, A. Terentjevs, F. Della Sala, P. Cortona, and E. Fabiano, Phys. Rev. B **93**, 045126 (2016).
[23] T. Van Voorhis and G. E. Scuseria, J. Chem. Phys. **109**, 400 (1998).
[24] J. Tao, J. P. Perdew, V. N. Staroverov, and G. E. Scuseria, Phys. Rev. Lett. **91**, 146401 (2003).
[25] J. P. Perdew, A. Ruzsinszky, G. I. Csonka, L. A. Constantin, and J. Sun, Phys. Rev. Lett. **103**, 026403 (2009).
[26] J. P. Perdew, A. Ruzsinszky, G. I. Csonka, L. A. Constantin, and J. Sun, Phys. Rev. Lett. **106**, 179902(E) (2011).
[27] J. Sun, B. Xiao, and A. Ruzsinszky, J. Chem. Phys. **137**, 051101 (2012).
[28] J. Sun, A. Ruzsinszky, and J. P. Perdew, Phys. Rev. Lett. **115**, 036402 (2015).
[29] Y. Zhao and D. G. Truhlar, J. Chem. Phys. **125**, 194101 (2006).
[30] J. Sun, B. Xiao, Y. Fang, R. Haunschild, P. Hao, A. Ruzsinszky, G. I. Csonka, G. E. Scuseria, and J. P. Perdew, Phys. Rev. Lett. **111**, 106401 (2013).
[31] F. Furche and T. Van Voorhis, J. Chem. Phys. **122**, 164106 (2005).
[32] J. F. Dobson, J. Wang, B. P. Dinte, K. McLennan, and H. M. Le, Int. J. Quantum Chem. **101**, 579 (2005).
[33] A. Heßelmann and A. Görling, Phys. Rev. Lett. **106**, 093001 (2011).
[34] J. M. Pitarke and A. G. Eguiluz, Phys. Rev. B **57**, 6329 (1998).
[35] J. M. Pitarke and A. G. Eguiluz, Phys. Rev. B **63**, 045116 (2001).
[36] J. M. Pitarke and J. P. Perdew, Phys. Rev. B **67**, 045101 (2003).
[37] J. M. Pitarke, Phys. Rev. B **70**, 087401 (2004).
[38] Z. Yan, J. P. Perdew, S. Kurth, C. Fiolhais, and L. Almeida, Phys. Rev. B **61**, 2595 (2000).
[39] L. A. Constantin, J. M. Pitarke, J. F. Dobson, A. Garcia-Lekue, and J. P. Perdew, Phys. Rev. Lett. **100**, 036401 (2008).
[40] B. Wood, N. D. M. Hine, W. M. C. Foulkes, and P. García-González, Phys. Rev. B **76**, 035403 (2007).
[41] D. C. Langreth and J. P. Perdew, Sol. State Comm. **17**, 1425 (1975).
[42] E. Runge and E. K. U. Gross, Phys. Rev. Lett. **52**, 997 (1984).
[43] D. C. Langreth and J. P. Perdew, Phys. Rev. B **21**, 5469 (1980).
[44] M. Lein, E. K. U. Gross, and J. P. Perdew, Phys. Rev. B **61**, 13431 (2000).
[45] M. Corradini, R. Del Sole, G. Onida, and M. Palummo, Phys. Rev. B **57**, 14569 (1998).
[46] L. A. Constantin and J. M. Pitarke, Phys. Rev. B **75**, 245127 (2007).
[47] C. F. Richardson and N. W. Ashcroft, Phys. Rev. B **50**, 8170 (1994).
[48] J. Paier, X. Ren, P. Rinke, G. E. Scuseria, A. Grüneis, G. Kresse, and M. Scheffler, New J. Phys. **14**, 043002 (2012).
[49] J. Harl and G. Kresse, Phys. Rev. Lett. **103**, 056401 (2009).
[50] C. E. Patrick and K. S. Thygesen, J. Chem. Phys. **143**, 102802 (2015).
[51] S. Lebegue, J. Harl, T. Gould, J. G. Ángyán, G. Kresse, and J. F. Dobson, Phys. Rev. Lett. **105**, 196401 (2010).
[52] L. Schimka, J. Harl, A. Stroppa, A. Grüneis, M. Marsman, F. Mittendorfer, and G. Kresse, Nature Materials **9**, 741 (2010).

[53] P. D. Mezei, G. I. Csonka, and A. Ruzsinszky, J. Chem. Theory Comput. **11**, 3961 (2015).
[54] B. Grabowski, S. Wippermann, A. Glensk, T. Hickel, and J. Neugebauer, Phys. Rev. B **91**, 201103 (2015).
[55] H. Eshuis, J. Yarkony, and F. Furche, J. Chem. Phys. **132**, 234114 (2010).
[56] J. Jung, P. Garcia-Gonzalez, J. F. Dobson, and R. W. Godby, Phys. Rev. B **70**, 205107 (2004).
[57] J. F. Dobson and J. Wang, Phys. Rev. B **62**, 10038 (2000).
[58] J. E. Bates, S. Laricchia, and A. Ruzsinszky, Phys. Rev. B **93**, 045119 (2016).
[59] L. A. Constantin and J. M. Pitarke, Phys. Rev. B **83**, 075116 (2011).
[60] C. v. Weizsäcker, Zeitschrift für Physik A Hadrons and Nuclei **96**, 431 (1935).
[61] M. Petersilka, U. J. Gossmann, and E. K. U. Gross, Phys. Rev. Lett. **76**, 1212 (1996).
[62] U. von Barth and L. Hedin, J. Phys. C: Sol. State Phys. **5**, 1629 (1972).
[63] L. H. Thomas, in *Mathematical Proceedings of the Cambridge Philosophical Society*, Vol. 23 (Cambridge Univ Press, 1927) pp. 542–548.
[64] E. Fermi, Rend. Accad. Naz. Lincei **6**, 32 (1927).
[65] A. Ruzsinszky, J. Sun, B. Xiao, and G. I. Csonka, J. Chem. Theory Comput. **8**, 2078 (2012).
[66] J. Sun, J. P. Perdew, and A. Ruzsinszky, Proceedings of the National Academy of Sciences **112**, 685 (2015).
[67] J. Wellendorff, K. T. Lundgaard, K. W. Jacobsen, and T. Bligaard, J. Chem. Phys. **140**, 144107 (2014).
[68] K. T. Lundgaard, J. Wellendorff, J. Voss, K. W. Jacobsen, and T. Bligaard, Phys. Rev. B **93**, 235162 (2016).
[69] F. Della Sala, E. Fabiano, and L. A. Constantin, Phys. Rev. B **91**, 035126 (2015).
[70] L. A. Constantin, E. Fabiano, J. M. Pitarke, and F. Della Sala, Phys. Rev. B **93**, 115127 (2016).
[71] B. Silvi and A. Savin, Nature **371**, 683 (1994).
[72] A. Savin, R. Nesper, S. Wengert, and T. F. Fässler, Angewandte Chemie International Edition in English **36**, 1808 (1997).
[73] J. P. Perdew and Y. Wang, Phys. Rev. B **45**, 13244 (1992).
[74] J. P. Perdew and Y. Wang, Phys. Rev. B **46**, 12947 (1992).
[75] J. Tao, V. N. Staroverov, G. E. Scuseria, and J. P. Perdew, Phys. Rev. A **77**, 012509 (2008).
[76] K. Burke, F. G. Cruz, and K.-C. Lam, J. Chem. Phys. **109**, 8161 (1998).
[77] K. Burke, F. G. Cruz, and K.-C. Lam, Int. J. Quantum Chem. **70**, 583 (1998).
[78] G. K. Madsen, L. Ferrighi, and B. Hammer, J. Phys. Chem. Lett. **1**, 515 (2009).